Mech. Sci., 2, 83–90, 2011
www.mech-sci.net/2/83/2011/
doi:10.5194/ms-2-83-2011

Mechanical Sciences
Open Access

Torque control of underactuated tendon-driven fingers

M. E. Abdallah and C. W. Wampler

General Motors R&D, Manufacturing Systems Research Lab, Warren, MI 48090, USA

Received: 26 February 2010 – Revised: 25 June 2010 – Accepted: 19 August 2010 – Published: 8 February 2011

Abstract. Given an underactuated tendon-driven finger, the finger posture is underdetermined and can move freely ("flop") in a region of slack tendons. This work shows that such an underactuated finger can be operated in tendon force control (rather than position control) with effective performance. The force control eliminates the indeterminate slack while commanding a parameterized space of desired torques. The torque will either push the finger to the joint limits or wrap around an external object with variable torque – behavior that is sufficient for primarily gripping fingers. In addition, introducing asymmetric joint radii to the design allows the finger to command an expanded range of joint torques and to scan an expanded set of external surfaces. This study is motivated by the design and control of the secondary fingers of the NASA-GM R2 humanoid hand.

This paper was presented at the IFToMM/ASME International Workshop on Underactuated Grasping (UG2010), 19 August 2010, Montréal, Canada.

1 Introduction

Tendon or cable transmission systems are often used in the actuation of fingers in high degree of freedom (DOF) hands. The remote actuation allows for significant reductions to the size and weight of the fingers, features that are important for dexterous manipulation. Since the tendons can only transmit forces in tension, the number of actuators must exceed the DOF's to achieve fully determined control of the finger. It turns out that only *one* tendon more than the number of DOF's is needed (Murray et al., 1994). If arranged correctly, the $n+1$ tendons can independently control the n DOF's while always maintaining positive tensions.

In this sense, an n-DOF finger with only n tendons is underactuated, and the finger posture is underdetermined. This creates a slack space within which the finger posture is uncontrolled. In other words, the finger cannot hold a desired position and will be free to flop in some region where the tendons go slack.

Despite this handicap, having a reduced number of actuators is still very attractive. Space or power limitations can be significant in high DOF hands. Each extra actuator and tendon transmission system increases the demands on space and maintenance. This work shows that an underactuated finger with n tendons can be operated in tendon force control (rather than position control) with effective performance. Desired joint torques can be commanded to the finger in a feasible torque space. The slack space is eliminated as the torques either push the finger to the joint limits or wrap around an external object. Others in the robotics community have applied tension control to tendon-driven hands, most notably for the Stanford/JPL, Utah/MIT, POSTECH, and Robonaut-2 hands (Salisbury and Craig, 1982; Biggers et al., 1986; Lee et al., 1994; Abdallah et al., 2010). In these cases, however, only fully actuated control strategies have been presented. Others have presented underactuated grippers, though they do not use force control (Hirose and Umetani, 1978) or spring load the joints to eliminate the slack space (Dollar and Howe, 2006).

The ability to independently control the joint torques depends on a finger design that has asymmetric joint radii. We shall discuss how the radii shape the feasible torque space. Furthermore, the asymmetric radii allow the finger to scan external surfaces whose target directions fall within a feasible set.

Correspondence to: M. E. Abdallah (muhammad.abdallah@gm.com)

Published by Copernicus Publications.

Figure 1. The secondary fingers of R2 are underactuated.

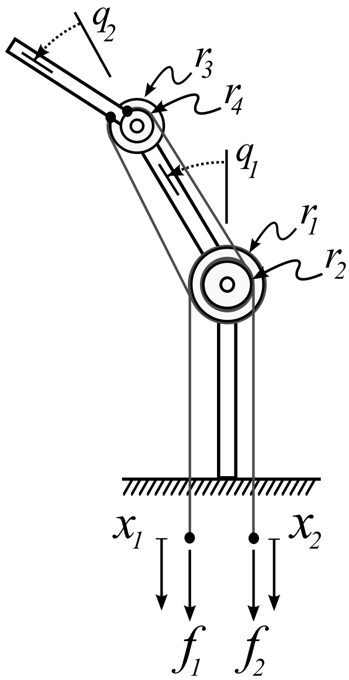

Figure 2. A 2 DOF finger with two tendons. x_1 represents the flexor tendon and x_2 the extensor.

In short, in asymmetric underactuated fingers, the torques are fully determined functions of the tendon tensions, whereas joint positions are not fully determined by the tendon positions. Therefore, we propose to control such fingers by controlling the tendon tensions instead of positions. This work starts with a thorough analysis of a two-DOF finger before generalizing the conditions to an n-DOF system.

This study was motivated by the design and control of the NASA-GM Robonaut-2 humanoid hand, shown in Fig. 1. The secondary fingers of the hand, i.e. the ring and little fingers, are underactuated to reduce the number of actuators and allow for a human-sized form factor. The primary objective of these fingers is to support the dexterous set of fingers in gripping larger objects.

2 Tension control

Suppose that we control the tensions in a tendon-actuated mechanism. For an open chain linkage with concentric circular pulleys and negligible friction, the relation between the actuated joint torques, $\boldsymbol{\tau}$, and tendon tensions, $\boldsymbol{f}$, is

$$\boldsymbol{\tau} = \mathbf{R}\boldsymbol{f}. \tag{1}$$

Matrix $\mathbf{R}$ is known as the tendon map matrix. If the pulleys are noncircular, the same relation holds, but $\mathbf{R}$ then varies with the configuration of the linkage. That is, if $\boldsymbol{q}$ is the set of joint angles for the linkage, we have $\boldsymbol{\tau} = \mathbf{R}(\boldsymbol{q})\boldsymbol{f}$. Although this relation is true for all tension values, one must remember that only non-negative tensions are possible. This limitation means that it is only feasible to access a limited portion of the joint torque space, as we will discuss further below.

As an illustration, consider the 2 DOF finger shown in Fig. 2. The tendons wrap around idler pulleys of radii r_1 and r_2 at the first joint, and radii of r_3 and r_4 at the second joint, terminating on the distal link. r_i are all positive scalars. In this case, the tendon map matrix becomes

$$\mathbf{R} = \begin{bmatrix} r_1 & -r_2 \\ r_3 & -r_4 \end{bmatrix}. \tag{2}$$

The dimensionality of the set of feasible torques depends on the design of the pulleys. For a symmetrical choice of pulley radii, $r_1 = r_2$ and $r_3 = r_4$, matrix $\mathbf{R}$ is singular. No matter what tensions are applied, the joint torques stay in a constant ratio $\tau_1/\tau_2 = r_1/r_3$. Thus, only a one-dimensional line in torque space is feasible, and this will be limited to just a line segment due to actuator saturation limits. In contrast, for a more general choice of radii, $\mathbf{R}$ becomes nonsingular, and we may invert Eq. (1) to obtain the tensions $\boldsymbol{f}$ that will produce a given joint torque $\boldsymbol{\tau}$:

$$\boldsymbol{f} = \mathbf{R}^{-1}\boldsymbol{\tau}. \tag{3}$$

Again, the limits on the tendon tensions give limits on what torques can be commanded. If $\mathbf{R}$ is nearly singular, even moderate torque commands in the singular direction will require large tensions. Nevertheless, there is a two-dimensional region of the torque space that is feasible.

3 Position control

Suppose that we control position of the tendons instead of their tensions. As long as the tendons remain taut, a standard virtual work argument implies that the relation between joint and actuator motion is governed by the same matrix $\mathbf{R}$ involved in the torque-tension relation (Eq. 1):

$$\dot{\boldsymbol{x}} = \mathbf{R}^T \dot{\boldsymbol{q}}, \tag{4}$$

where $\boldsymbol{x}$ is the set of tendon actuator positions. In the more general case where the tendons may become lax, it is helpful to introduce an intermediate variable $\boldsymbol{y}$ that represents the tendon extension that would keep the tendons taut, while $\boldsymbol{x}$ is the actual extension of the tendon actuators. Then, starting from any configuration in which the tendons are initially taut, i.e., $\boldsymbol{x} = \boldsymbol{y}$, we have

$$\dot{\boldsymbol{x}} \leq \dot{\boldsymbol{y}} = \mathbf{R}^T \dot{\boldsymbol{q}}. \tag{5}$$

(By this notation, we mean that the inequality holds for each row of the matrix expression.) Even if the actuators are held stationary, $\dot{\boldsymbol{x}} = 0$, the finger can move with $\dot{\boldsymbol{y}}$ in the positive quadrant: $\dot{y}_1 \geq 0$, $\dot{y}_2 \geq 0$. Such motions enter the *slack region*, a bounded region in which the finger may move freely even though the actuators are held stationary.

The slack region is described by inequalities at the position level. We assume that all quantities are measured from an initial position $\boldsymbol{x} = \boldsymbol{y} = \boldsymbol{q} = 0$ in which the tendons are taut. Assuming inelastic tendons, the joint motion is constrained by the length of tendons:

$$\boldsymbol{x} \leq \boldsymbol{y} = \mathbf{R}^T \boldsymbol{q}. \tag{6}$$

In particular, for the finger of Fig. 2, we have

$$\begin{aligned} x_1 &\leq r_1 q_1 + r_3 q_2 \\ x_2 &\leq -r_2 q_1 - r_4 q_2 \end{aligned} \tag{7}$$

In general, the intersection of these two inequalities consists of a wedge that defines the slack region. As the input side of the tendons (x_1 and x_2) are displaced, these inequalities shift and change the slack region. An example is shown in Fig. 3. In the interior of the slack region, the tendons lose tension, while on either boundary, one tendon is taut, the other slack. For symmetric designs, the constraints become parallel as shown in Fig. 4. In this case, the tendons perfectly oppose each other, so they can be drawn taut, at which point their constraints in joint space collapse onto each other into a single line that matches the null-space of $\mathbf{R}^T$. Even though the tendons will remain taut, they cannot resist motion along this line.

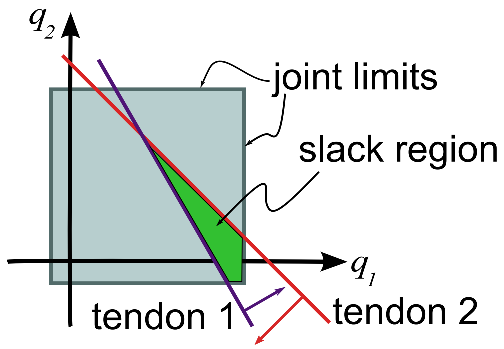

Figure 3. The slack space (shaded region) is bound by the two constraints (lines) and the joint limits (box).

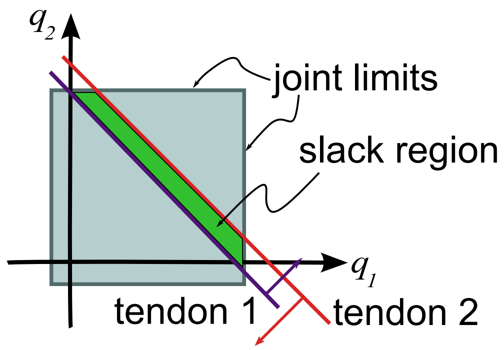

Figure 4. The slack space for a symmetric pulley design.

4 Feasible torques

Not all joint torques are possible due to the nature of both the tendons and actuators. Due to the tendons, each tendon tension f_i, $i = 1, \ldots, n$, must be nonnegative. Due to the actuators, each tendon tension also has an upper limit, say f_i^+. In short,

$$0 \leq f_i \leq f_i^+, \qquad i = 1, \ldots, n. \tag{8}$$

This rectangular region in tension space gets mapped by $\mathbf{R}$ into an n-parallelotope (the generalization to n dimensions of a parallelogram.) The 2^n vertices of this feasible torque region are given by evaluating $\mathbf{R}\boldsymbol{f}$ for every combination of tendon tensions at their respective limits. In particular, let $\boldsymbol{R_i}$ be the i-th column of $\mathbf{R}$. Then, for a two-link finger actuated by two tendons, the feasible torque region is a parallelogram with vertices:

$$\{(0,0), \boldsymbol{R}_1 f_1^+, \boldsymbol{R}_2 f_2^+, \boldsymbol{R}_1 f_1^+ + \boldsymbol{R}_2 f_2^+\}.$$

Figure 5 illustrates the case of $r_1 > r_2 = r_3 = r_4$ with equal maximum tensions.

It is appropriate to limit the finger operation to the condition that both joint torques have the same direction. In other words, the joints are both in either flexion or extension. This covers the behavior of fingers designed for gripping. In Fig. 5, the regions that correspond to this condition

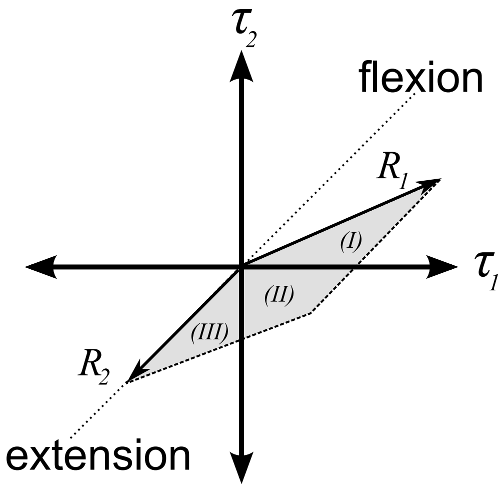

Figure 5. The space of feasible joint torques. It represents the positive span of $\boldsymbol{R}_i$, given upper bounds on the tensions. Region (I) indicates when both joints are in flexion. Region (III) indicates when both joints are in extension.

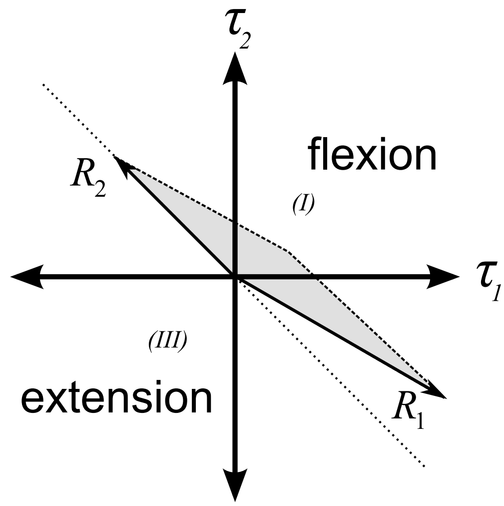

Figure 6. A different tendon arrangement can produce undesirable results. In this case, both joints cannot be extended simultaneously.

are regions I and III. Hence in flexion, $\tau_2 \leq \frac{r_1}{r_2}\tau_1$. While in extension, $\tau_2 \leq \tau_1$.

For the sake of simplicity, the joint torques in the two-joint finger can also optionally be limited to operate along just $\boldsymbol{R}_1$ or $\boldsymbol{R}_2$, that is, we pull on one tendon while maintaining a minimal tension on the other. In this case, the torques become parameterized by a single DOF. This mode of operation causes the joint torques to be both in either flexion or extension. Such a control mode is well suited for fingers designed primarily for gripping. While fingers intended for manipulation need to be fully actuated and fully controllable, gripping fingers simply need to flexibly grip objects with variable strength and variable posture. Hence, one DOF is sufficient to either specify the grip strength or to fully extend the finger. The commanded joint torques will thus drive the finger until it either comes to rest against the joint limits or wraps around an external object.

5 Design considerations

The tendon configuration greatly affects the feasible joint torque space, and a bad design can produce a space with undesirable characteristics. Consider the same finger in Fig. 2, but suppose we reverse the direction of wrap on the upper joint. This results in a new tendon map,

$$\mathbf{R} = \begin{bmatrix} r_1 & -r_2 \\ -r_3 & r_4 \end{bmatrix}. \tag{9}$$

Although this arrangement is valid in many ways, it produces a potentially undesirable space of feasible joint torques – shown in Fig. 6. Assuming $r_1 > r_2 = r_3 = r_4$, as before, the feasible region excludes quadrant three, meaning that the finger can no longer command both joints simultaneously in extension, and its ability to simultaneously move both in flexion is limited.

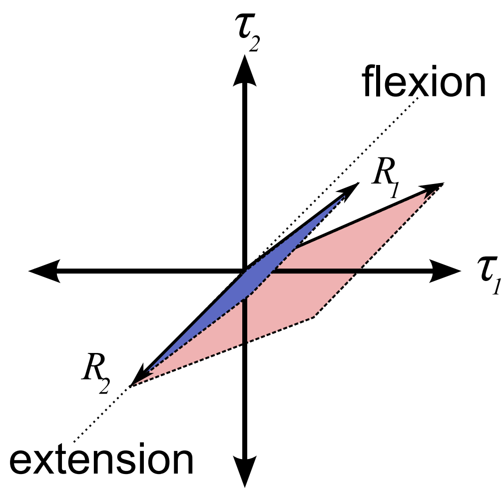

Figure 7. For limited tendon tensions, the torque space is defined by the above parallelogram. The ratio of $\frac{r_1}{r_2}$ affects the area and conditioning of the possible solution.

The size of the joint radii carry several design implications as well. For a given tendon force and stroke length, larger radii increase the maximum joint torques while decreasing the joint range. Consider Fig. 5 again. To obtain good control off the diagonal, the differences in the radii must be large enough to leave $\mathbf{R}$ well conditioned. As r_1 increases with $r_2 = r_3 = r_4$, vector $\boldsymbol{R}_1$ rotates clockwise and grows in length. As $\boldsymbol{R}_1$ rotates, the area of the feasible parallelogram increases, but the ability to move along the diagonal in flexion is sacrificed. This behavior is demonstrated in Fig. 7.

It is important to note that while a more asymmetrical arrangement increases the area of the feasible torque region, it also widens the slack region. This is not too much of a concern as long as the finger is under tension control, or if the actuators are parked near a boundary of the joint space (see next section). But if the actuators are parked in the middle of their ranges, the larger slack region may be undesirable. For example, it may be possible for slack tendons to escape their guideways such that the mechanism will not return to a usable state even when the actuators re-tension the tendons.

6 Position control with external constraints

We have seen that position control of an underactuated finger can only constrain the finger to a slack region. Without joint limits or external contact constraints, this region would be infinite in extent, but with them, the slack region becomes finite. In fact, under certain conditions, the slack region can shrink to a point, that is, the underactuated finger can become fully controlled in position when acting against a constraint.

It takes a minimum of three inequalities to bound a finite region of the plane, or in general, $n+1$ inequalities to bound a finite region in n-space. This is the fundamental reason why $n+1$ tendons are required to hold an n-DOF mechanism in place without any external constraints. But once the mechanism contacts the environment or a hard joint limit, its freedom drops and n tendons may become sufficient. However, the direction of the external constraint matters: it must be oriented such that the finger can exert a positive force against it. It is easiest to understand this if the external constraint is first mapped into an equivalent joint-space constraint. Then the ability to exert forces on the constraint can be reinterpreted as the ability to exert joint torques against the joint space constraint.

The symmetric pulley case, or any case in which $\mathbf{R}$ has co-rank 1 (meaning that it is singular with a one-dimensional null space), there remains a complete one-dimensional slack space. Any single one-sided constraint can only cut this infinite line into a ray. It takes two independent constraints in opposition to reduce the slack region to a single point. We illustrate this in the next section on joint limits.

6.1 Joint limits

Let's first examine the situation for the case of joint limit constraints without additional contact. Figure 3 shows the slack region for the two-joint finger with asymmetric radii. Notice that if the tendons are pulled sufficiently, the slack region will shrink to a point somewhere on the boundary of the joint limit box. Figure 8 illustrates a configuration where the slack region has been reduced to a tiny triangle. A slight additional tug on either tendon will trap the finger at a point with q_1 at its maximum, q_1^+. It is clear that in this manner the finger can be fully constrained at any point on the southeast boundary of the joint limits, that is, any point with either q_1 at its maximum q_1^+ or q_2 at its minimum q_2^-.

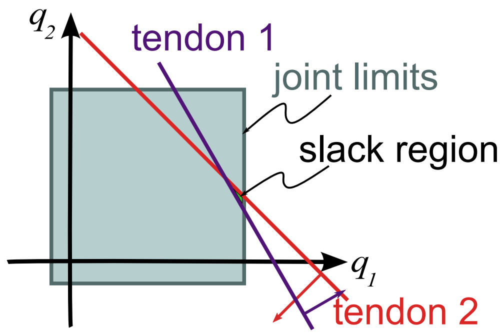

Figure 8. The asymmetric finger trapped near the maximum of q_1.

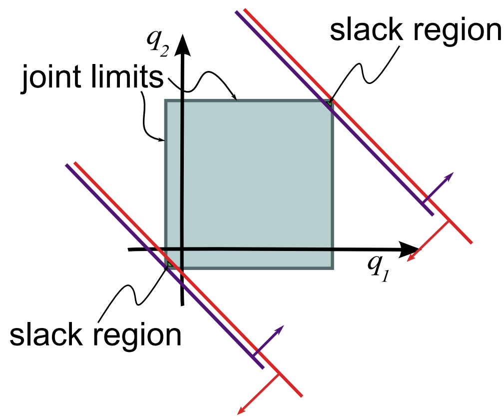

Figure 9. The symmetric finger is stable only at full flexion or full extension.

In contrast, the symmetric finger requires two additional constraints to become fully constrained. This can occur only at full flexion (q_1 and q_2 both at their maxima) or at full extension (both joints at their minima). This is illustrated in Fig. 9.

Another way to view the situation is through the feasible torque space. By reference to Fig. 5, one sees that the asymmetric finger can generate torque in either the positive τ_1 or the negative τ_2 directions and can also generate torque vectors with components that can resist movement along the $q_1 = q_1^+$ or the $q_2 = q_2^-$ joint limits. In contrast, the symmetric arrangement can only generate torques along the diagonal, $\tau_1 = \tau_2$, and thus can be stably driven only to the corners along this diagonal.

6.2 General constraints

Point contact with an external object introduces a new constraint and multiple point contacts introduce multiple constraints. These may be mapped into the joint space of the mechanism. Neglecting friction, the mechanism may reach quasi-static equilibrium in contact if and only if the inward normal to the contact constraint in joint space is within the

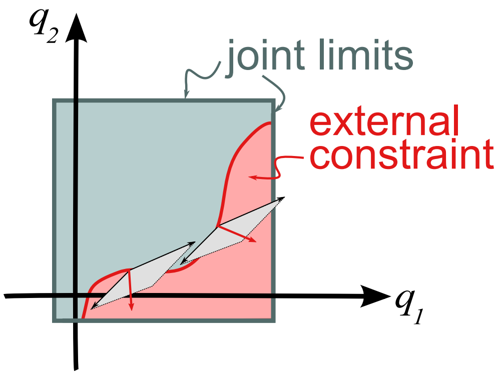

Figure 10. Equilibrium conditions for a asymmetric finger touching a general constraint. Constraint inner normal (red) is directed into the superimposed feasible torque region.

set of feasible torques. In other words, the robot must be able to exert positive force along the normal to the constraint.

For our example of the 2-DOF finger, it is convenient to visualize this by overlaying the feasible torque diagram, Fig. 5, onto the constraint curve in joint space, as shown in Fig. 10. In the figure, the feasible torque region has been superimposed at two different points along the contact constraint curve. Since the inner normal at those points are directed into the feasible torque region, a positive contact force can be applied normal to the constraint and equilibrium is possible.

We note that if friction is present, then the range of slopes for the constraint curve where stable contact is possible expands. By the same token, since friction impedes the finger from sliding along the constraint, the range of slopes along which the finger can be driven along the constraint decreases.

If the finger is close to the symmetric design, the magnitude of the torque vector that can be generated perpendicular to the main diagonal is greatly diminished. Suppose that the constraint runs along the main diagonal. Even though in principle the finger can produce a force normal to the constraint, it can at best exert a small force towards it, and this will be further diminished by any friction in the mechanism. Furthermore, the torque vectors $\boldsymbol{R}_1$ and $\boldsymbol{R}_2$ are nearly opposed, so the direction of the resultant torque is highly sensitive to small errors in the tendon forces. For the finger to be well-controlled in sliding contact along such a constraint, its design must be sufficiently asymmetric to give a well-conditioned tendon map matrix $\mathbf{R}$.

So far, we have visualized the constraints only in the joint space. One may also consider the equivalent picture at the contact point. Let $\boldsymbol{v}$ be the velocity of the contact point and let $\boldsymbol{F}$ be the force exerted on the environment by the finger at the contact point. We have the usual velocity and force relations:

$$\mathbf{J}\dot{\boldsymbol{q}} = \boldsymbol{v}, \qquad \boldsymbol{\tau} = \mathbf{J}^T \boldsymbol{F}, \tag{10}$$

where $\mathbf{J}$ is the Jacobian for the contact point. From these and Eq. (1),

$$\boldsymbol{F} = \mathbf{J}^{-T}\mathbf{R}\boldsymbol{f}. \tag{11}$$

Thus, in operational space, the columns of $\mathbf{J}^{-T}\mathbf{R}$ play the analogous role as the columns of $\mathbf{R}$ play in building the feasible torque region. The external constraints that can be stably contacted with a single point contact are those whose inward normal lies within the positive range space of $\mathbf{J}^{-T}\mathbf{R}$.

Two-point contact is another matter. This may occur when the fingertip is inserted into a corner feature or it may occur when the inner and outer phalanges each contact an object within a grasp. Now, the constraints give two inward normals in the joint-space diagram and the finger gives the two vectors $\boldsymbol{R}_1$ and $\boldsymbol{R}_2$, as usual. Each of these defines a feasible parallelogram, and as long as there is an overlap between them, there exists sets of tendon forces that stably direct the finger into the constraint.

7 Higher DOF fingers

Although we have illustrated all the above concepts on a 2-DOF finger, they apply equally well on any n-DOF manipulator controlled by n tendons. We discuss here some of the subtleties of the general case.

The feasible torque space, i.e. the positive range space of $\mathbf{R}$, determines what kind of constraints can be stably contacted. Suppose we consider only joint limits. If $\mathbf{R}$ has n independent columns, i.e., if it is nonsingular, then it takes only 1 additional constraint to reach an equilibrium among the total of $n+1$ forces, all nonzero. Accordingly, any face of the joint limit polytope is a candidate for stable positioning. However, we need the additional fact that all the tendon forces are positive and the net torque is directed along the inward normal of the joint limit constraint (which is to say, an outward normal of the limit polytope). Only certain faces are oriented such that this is possible. Let $\boldsymbol{e}_i$ be an elementary vector with 1 in the i-th position and zeros elsewhere. Then, the mechanism can achieve equilibrium on the positive $\boldsymbol{e}_i$ face of the joint limits if and only if there is an all positive solution $\boldsymbol{f}$ of

$$\boldsymbol{e}_i = \mathbf{R}\boldsymbol{f}, \tag{12}$$

or in other words, if $\mathbf{R}^{-1}\boldsymbol{e}_i$ has all positive elements. When this condition is satisfied, we will say that the face is "stable". The opposing face in the $-\boldsymbol{e}_i$ direction is stable if and only if $-\mathbf{R}^{-T}\boldsymbol{e}_i$ is all positive, which means that only one of two opposing faces can be stable.

Where two faces meet, that is, on a $(n-2)$-dimensional "edge" of the joint limit polytope, equilibrium is possible if at least one of the faces is stable. However, there is an additional freedom to exert forces on both faces simultaneously, hence the condition to be stable on the edge where the $\boldsymbol{e}_i$ and

$\boldsymbol{e}_j$ faces meet is that there must exist an all positive solution $(\lambda_i, \lambda_j, \boldsymbol{f})$ to

$$\boldsymbol{e}_i \lambda_i + \boldsymbol{e}_j \lambda_j = \mathbf{R} \boldsymbol{f}. \tag{13}$$

(The obvious sign adjustment is made for a face in the $-\boldsymbol{e}_i$ direction.) Accordingly, write the solution for $\boldsymbol{f}$ in terms of $\boldsymbol{\lambda} = (\lambda_i, \lambda_j)^T$ as

$$\boldsymbol{f} = \left[\mathbf{R}^{-1}\boldsymbol{e}_i \quad \mathbf{R}^{-1}\boldsymbol{e}_j \right] \boldsymbol{\lambda} = W \boldsymbol{\lambda}. \tag{14}$$

If either column is all positive, there is an all positive solution for $\boldsymbol{f}$. If any row of W is all negative, then there is no all-positive solution. All positive rows give a positive left-hand side no matter what positive $\boldsymbol{\lambda}$ is used. So the only problems are the rows with one positive and one negative entry. To this end, consider the 2×2 system

$$\boldsymbol{w} = \begin{bmatrix} a & -b \\ -c & d \end{bmatrix} \boldsymbol{\lambda}, \tag{15}$$

where a,b,c,d are all positive. It is easy to show that there is an all-positive solution $(\boldsymbol{w}, \boldsymbol{\lambda})$ if and only if

$$d/c > b/a. \tag{16}$$

This must be true for every 2×2 minor of W. So scanning the rows of W, one picks out the smallest d/c and the largest b/a. If these satisfy Eq. (16), then the edge is stable. Notice that it is possible for the edge to be stable even if neither of the adjoining faces is.

It is more difficult to assess lower-dimensional facets. However, let's examine the extreme case of a vertex. In particular, let's consider the vertex where all joints are at their upper limits. Hence, the question of stability comes to the existence of an all-positive solution to

$$I \boldsymbol{\lambda} = \mathbf{R} \boldsymbol{f}. \tag{17}$$

If $\mathbf{R}$ has an all-positive column, then this equation has all-positive solutions. However, this is a sufficient but not necessary condition, as is clear from the discussion on edges above. In general, the question of whether an all-positive solution exists has no simple solution, but the question can always be answered using the techniques of Linear Programming. As in the $(n-2)$ dimensional edge case above, it is clearly necessary that every row of $\mathbf{R}$ have at least one positive element; otherwise the associated element of $\boldsymbol{\lambda}$ is always negative for nonzero positive $\boldsymbol{f}$. If we also want the opposing vertex where all joints are at their minima to be a stable point, then we need an all-positive solution to $-I\boldsymbol{\lambda} = \mathbf{R}\boldsymbol{f}$, or equivalently, $\boldsymbol{\lambda} = (-\mathbf{R})\boldsymbol{f}$. So the same logic that applies to $\mathbf{R}$ in the former case now applies to $-\mathbf{R}$.

Although the condition of an all-positive column is not necessary, it does offer a simple condition for the design of a basic gripper finger. For a finger designed to wrap around an external object in one direction and fully extend in the other direction, it suffices for $\mathbf{R}$ to have one all-positive and one all-negative column.

8 Conclusions

We have examined possible design and control trade-offs for underactuated tendon-driven mechanisms, in particular, n-DOF mechanisms driven by only n tendons. One would like to operate a tendon-driven mechanism without allowing slack in any tendon. One would also like to reliably drive the mechanism to certain configurations where the mechanism will be in stable equilibrium. Finally, when the mechanism is in contact with the environment, one might like to be able to move the contact point along the environmental obstacle. This article examines the trade-offs between these objectives as they depend on the tendon map matrix $\mathbf{R}$ that relates tendon tensions to joint torques. Our objective is to present the fundamental ideas, including the idea of a slack region and torque controllability. To keep the analysis simple, we ignore friction, which may occur in the finger joints and tendon transmission elements, and we assume inelastic tendons. There would be value in developing more a sophisticated analysis that includes these neglected effects.

Mechanisms can be classified according to whether $\mathbf{R}$ is singular or nonsingular. In the singular case, we assume $\mathbf{R}$ has rank $n-1$, leaving a one DOF null-space. ($\mathbf{R}$ with lower rank are not practically useful.) If the elements of this null vector are all of the same sign, then the tendons can all be in tension without generating any torque at the joints. Although this is a desirable characteristic, it comes at a price: the mechanism also has a 1-dimensional slack region that is limited only by the joint limits of the mechanism. To reach a stable equilibrium, the mechanism must meet up with at least two obstacles, either two joint limits or two point contacts with the environment (or one of each).

By choosing $\mathbf{R}$ to be nonsingular, the set of feasible torques becomes an n-dimensional parallelotope (a parallelogram in the case of $n=2$). One can drive the mechanism in any direction within the positive range space of $\mathbf{R}$. The slack region changes to a cone extending from the point where all tendons are taut. If one locks the actuators in place, the mechanism can freely move within this cone and the tendons lose tension. On the good side, the motion is limited in the sense that it cannot go beyond the vertex of the cone. This characteristic is valuable, and it gives the mechanism the capability of reaching a stable equilibrium with only a single point of contact or a single joint limit.

These concepts are examined thoroughly in the case of a 2-DOF finger. It is shown that to get a nonsingular $\mathbf{R}$ that can both flex and extend the finger, then at least one pulley radius must be different than the others. We call this an asymmetrical design. We illustrate how the asymmetric finger can be fully flexed and fully extended and also can move along two of four boundaries where one joint is at a limit. It can also scan some external obstacles. We detail how to tell which joint limits and which obstacle shapes can be scanned in quasi-static equilibrium. In contrast, a symmetric finger can only come to equilibrium when trapped at the intersection of two constraints: it cannot move in quasi-static equilibrium.

We also outline how to analyze the capabilities of mechanisms with more than two joints by an examination of the **R** matrix.

Edited by: J. L. Herder
Reviewed by: two anonymous referees

References

Abdallah, M. E., Platt, R., Wampler, C. W., and Hargrave, B.: Applied Joint-Space Torque and Stiffness Control of Tendon-Driven Fingers, in: IEEE Intl. Conf. on Humanoid Robots, Nashville, TN, 2010.

Biggers, K., Jacobsen, S., and Gerpheide, G.: Low level control of the Utah/M.I.T. dextrous hand, in: The IEEE International Conference on Robotics and Automation (ICRA), 61–66, 1986.

Dollar, A. and Howe, R.: Joint Coupling Design of Underactuated Grippers, in: Proceedings of ASME Intl. Design Engineering Technical Conferences, Philadelphia, PA, 1–9, 2006.

Hirose, S. and Umetani, Y.: The development of soft gripper for the versatile robot hand, Mech. Mach. Theory, 13, 351–359, 1978.

Lee, Y., Choi, H., Chung, W., and Youm, Y.: Stiffness Control of a Coupled Tendon-Driven Hand, IEEE Contr. Syst. Mag., 14, 10–19, 1994.

Murray, R., Li, Z., and Sastry, S.: A Mathematical Introduction to Robotic Manipulation, CRC Press, Boca Raton, FL, 1994.

Salisbury, J. and Craig, J.: Articulated hands: Force control and kinematic issues, Int. J. Robot. Res., 1, 4–17, 1982.